Available online at www.sciencedirect.com
ScienceDirect
Tetrahedron
Tetrahedron 63 (2007) 7302–7308

Supramolecular hydrogel formed by glucoheptonamide of L-lysine: simple preparation and excellent hydrogelation ability

Masahiro Suzuki,* Sanae Owa, Hirofusa Shirai and Kenji Hanabusa*

Graduate School of Science and Technology, Shinshu University, Ueda, Nagano 386-8567, Japan

Received 16 October 2006; revised 5 February 2007; accepted 9 February 2007
Available online 20 February 2007

Abstract—We describe the simple preparation of new L-lysine derivatives with a gluconic or glucoheptonic group, their hydrogelation properties, and the thermal and mechanical properties of the supramolecular hydrogels. The L-lysine derivatives with a gluconic group have no hydrogelation ability, while the L-lysine-glucoheptonamide derivatives functioned as hydrogelators. Their hydrogelation abilities increased with the decreasing length of the spacer between the L-lysine segment and the glucoheptonic group. The compound, which has no spacer, formed a supramolecular hydrogel at 0.05 wt % in pure water. The thermal stability and high mechanical strength of the supramolecular hydrogels based on this compound significantly depended on the aqueous solutions. Electron microscopy and FTIR studies demonstrated that the hydrogelators created a three-dimensional network through hydrogen bonding and hydrophobic interactions in the supramolecular hydrogel. In addition, it was found that hydrophobic interactions played an important role in the thermal stability of the supramolecular hydrogel.

1. Introduction

Over recent years, low-molecular weight hydrogelators have become an area of considerable interest, involving the development of low-molecular weight organogelators.[1–21] In a supramolecular gel, gelators self-assemble into nano-scale supramolecular polymers with the monomer units being linked via noncovalent interactions such as hydrogen bonding, van der Waals, π–π stacking, coordination, and electrostatic interactions. Therefore, the supramolecular polymers show polymeric properties in solution and in the bulk. Because of the reversible dynamic conversion from supramolecular polymers to monomers by external stimuli such as temperature, pH, ionic strengths, light, and electricity, gelators are useful as new soft materials alternative to conventional polymers. Based on the gelation behavior of organic solvents by an organogelator, many hydrogelators have subsequently been reported.[6–21] The molecular structures of hydrogelators are designed based on those of organogelators. The important points for the conversion of organogelators into hydrogelators are: (i) to be water-soluble and (ii) to keep the self-assembling properties of organogelators intact. One of the simplest strategies is the introduction of charges into the terminus of organogelators. According to this strategy, we have developed L-amino acid-based hydrogelators with a positively or negatively charged terminal group; in particular, the positively charged hydrogelators based on L-lysine, L-valine, and L-isoleucine function as excellent hydrogelators that can form hydrogels below 0.5 wt %.[9,22–26] Another strategy for hydrogelators is the introduction of nonionic water-soluble functional groups such as sugars, nucleotides, hydroxyl groups, and aldonamides.[1–3,5,14,27–35] In this paper, we describe a new class of hydrogelators based on L-lysine derivatized with aldonamide.

2. Results and discussion

The synthetic procedures are illustrated in Scheme 1.[36] The amino group of amino acids (6-amino-1-hexanoic acid or 12-amino-1-dodecanoic acid) was protected with a benzyloxycarbonyl group, and then the amino-protected amino acids were converted into the acid chlorides using oxalyl chloride in dry dichloromethane. After reaction of the acid chlorides with N^{ε}-lauroyl-L-lysine ethyl ester,[9] the amino group-terminated L-lysine derivatives were obtained by deprotection using Pd/C. Finally, compounds **1** and **2** were obtained by the reaction with D-(+)-glucono-1,5-lactone or D-glucoheptono-1,4-lactone in methanol. Compounds **3a** and **3b** were simply prepared from N^{ε}-lauroyl-L-lysine ethyl esters and lactones in methanol.

As mentioned above, we have reported some positively charged L-lysine hydrogelators; especially, N^{α}-(11-pyridinium undecanoyl)-N^{ε}-dodecaonyl-L-lysine ethyl ester bromide (**A**) is an excellent hydrogelator that can form

* Corresponding authors. Tel.: +81 268 21 5415; fax: +81 268 21 5608; e-mail: msuzuki@giptc.shinshu-u.ac.jp

0040–4020/$ - see front matter © 2007 Elsevier Ltd. All rights reserved.
doi:10.1016/j.tet.2007.02.065

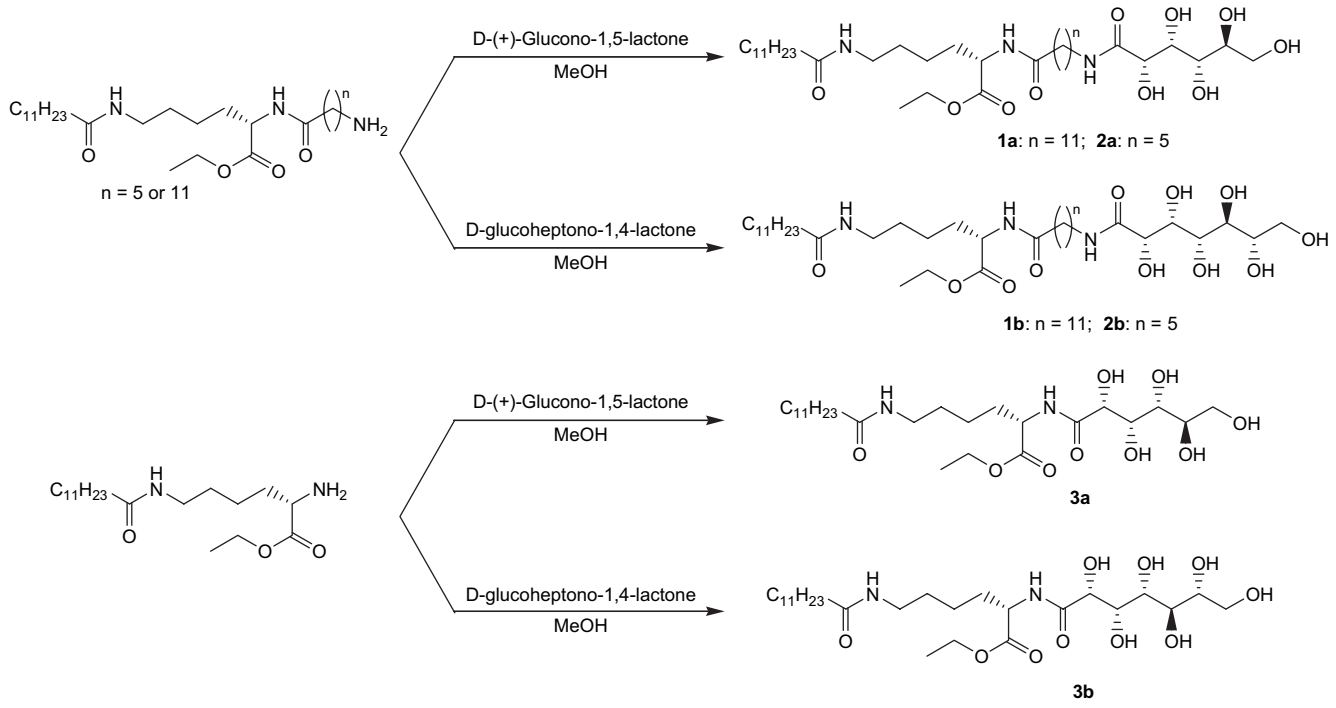

Scheme 1. Synthetic procedure for L-lysine aldonamide derivatives.

a hydrogel at 3 g L^{-1} (Fig. 1).[9,23] In contrast, compound **B** had no hydrogelation ability. Based on this hydrogelator, we prepared compounds **1a** and **1b**, which had a nonionic and hydrophilic group at the terminal, and examined their hydrogelation abilities. Compound **1a** was water-insoluble and did not act as a hydrogelator, while **1b** formed a hydrogel at 15 g L^{-1}. It is noteworthy that the increase in number of only one hydroxyl group brings about water-solubility and hydrogelation ability. Compared with compound **A**, the hydrogelation ability of **1b** was relatively low because its hydrophilic–hydrophobic balance was unsuitable. For compounds **1a**–**3a**, possessing a gluconic group (five hydroxyl groups), these compounds did not function as hydrogelators; compounds **1a** and **2a** were water-insoluble and compound **3a** precipitated after dissolution in water. This is attributed to the lack of hydrophilicity of the gluconic head group, which leads to the unsuitable hydrophilic–hydrophobic balance. On the other hand, compounds **1b**–**3b**, possessing a glucoheptonic group (six hydroxyl groups), functioned as hydrogelators. Surprisingly, **3b** was an excellent hydrogelator that formed a transparent hydrogel at 0.5 g L^{-1} corresponding to one gelator molecule immobilizing more than 62,000 water molecules (for hydrogelator **A**, ca. 12,600 water molecules were immobilized)[9,23] (Table 1).

For the positively charged L-lysine-based hydrogelator system, the hydrogelation ability was lost when the length of the alkylene spacers between the L-lysine segment and

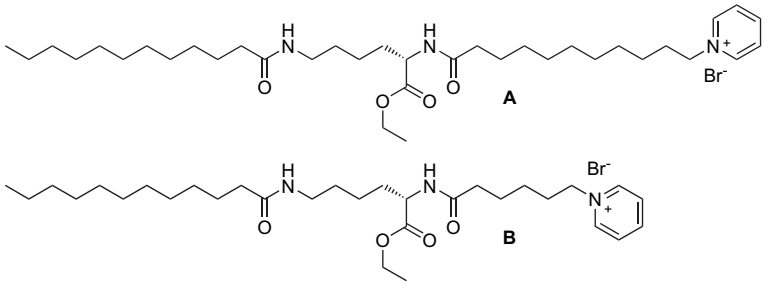

Figure 1. Positively charged L-lysine derivatives.

Table 1. Hydrogelation properties of **1–3** in pure water at 25 °C

	1a	2a	3a	1b	2b	3b
Pure water	Insoluble	Insoluble	Precipitate	15[a]	5[a]	0.5[a]
H_2O molecules[b]	—	—	—	2820	7520	62,670

[a] Minimum gel concentration necessary for hydrogelation (MGC, g L^{-1}).
[b] The number of water molecules that is immobilized by one gelator molecule.

pyridinium group decreased; indeed, compound **B** did not function as a hydrogelator. In the present case, the hydrogelation ability decreased with the increasing number of carbons in the alkylene spacer between the L-lysine segment and the glucoheptonic group (i.e., increase in hydrophobicity). This is ascribed to a difference in hydrophilicity of the terminal group; probably, the glucoheptonic group has less hydrophilicity than the positively charged pyridinum.

The hydrogelation abilities of **1b–3b** were examined in aqueous solutions of various pHs, which were adjusted by HCl (pH=0–6) or NaOH (pH=8–14) and the results are listed in Table 2. Although **1b** was insoluble in aqueous solutions with the high concentrations of HCl (>0.01 M) and NaOH (>0.001 M), it formed a hydrogel in aqueous solutions with pH=2–10. Compound **2b** gelled aqueous solutions with pH=0–10. Compound **3b** formed a hydrogel in aqueous solutions of pH=0–12 below 4 g L^{-1}, while it was not able to form a hydrogel with high concentrations of alkali (pH≥13). The hydrogels prepared from alkali solutions of pH=9–12 had a short lifetime and collapsed within 2 weeks; especially, the hydrogel of pH=12 based on **3b** collapsed one day later. The FTIR spectrum of the precipitate showed that the IR peak of the ester group was no longer observed. This fact implies that the collapse of hydrogels formed by alkali solutions is caused by hydrolysis of the ester group. In contrast, the hydrogels prepared from aqueous solutions of pH=1–8 have very long lifetimes and are stable for more than half a year. Similar results were obtained using other acids such as sulfuric acid, phosphoric acid, and acetic acid. Therefore, **2b** and **3b** form an acid-resistant hydrogel.

Table 3 lists the hydrogelation properties of **1b–3b** in aqueous solutions containing 1 M acids and salts. Although **1b** was insoluble in saline and aqueous solutions containing 1 M inorganic acids and salts, it formed a hydrogel in acetic acid solution at 2 g L^{-1}. It is noteworthy that the MGC value is greater than that in pure water. Except for the $CaCl_2$ solution, **2b** formed a hydrogel in all the aqueous solutions and their MGC values were barely affected by the addition of inorganic salts and acids. In the presence of inorganic salts, however, the hydrogelation ability tends to slightly decrease. In contrast, inorganic salts and acids influenced the hydrogelation ability of **3b**. The MGC values increased in the presence of these additives; especially, the MGC values for HCl and $CaCl_2$ solutions are 8 times larger than those for pure water. In summary, compound **3b** can form a hydrogel containing a high concentration of ions such as protons, alkali ions, alkali earth metal ions, and anions below 0.5 g L^{-1} of the gelator, it is an excellent hydrogelator.

Compound **3b** formed transparent or translucent hydrogels in these aqueous solutions, e.g., giving transparent hydrogels for pure water and acid solutions, while giving translucent hydrogels for inorganic salt solutions. It is well-known that a supramolecular gel is often formed by self-assembled nanofibers.[1–5] The superstructures created by the gelators in the hydrogels were observed using a transmission electron microscope (TEM). Figure 2 shows the photographs of hydrogels and TEM images of their dried gels prepared from pure water gel, saline gel, and NaCl gel based on **3b**. The pure water gel was transparent, while the saline and NaCl gels were translucent. The TEM images demonstrate a three-dimensional network formed by the entangling self-assembled nanofibers of the hydrogelators. The average diameters of self-assembled nanofibers are about 10–50 nm for the pure water gel, 30–100 nm for saline gel, and 60–150 nm for 1 M NaCl gel. These results correspond with the aspects of hydrogels; the nanofibers in the transparent hydrogel are smaller to those in the translucent hydrogels.[23]

The evidence for the intermolecular interactions between the gelator molecules in the gel state was provided by FTIR analysis. As shown in Figure 3A, the FTIR spectrum of the D_2O gel (at 25 °C) showed the typical peaks at 1632 cm^{-1} and at 1677 cm^{-1}. Such a characteristic IR spectrum demonstrates that the self-assembled nanofibers are formed through an intermolecular hydrogen bonding interaction between the amide groups and have an antiparallel β-sheet arrangement.[37,38] The CD spectrum of the D_2O gel showed a negative peak at 202 nm and shoulder at 216 nm. This CD result supports the IR data. In addition, the absorption bands of antisymmetric (ν_{as}) and symmetric (ν_s) C–H stretching vibrations were observed at 2920 cm^{-1} (ν_{as}C–H) and 2850 cm^{-1} (ν_sC–H), and in the IR region arising from the amide A and hydroxyl group, the IR peak appeared at 3400 cm^{-1}.[36] On the other hand, at 80 °C (solution), the IR spectrum and CD spectrum drastically changed; the long wavenumber shifts of νC–H (2920 cm^{-1} → 2925 cm^{-1} and 2850 cm^{-1} → 2855 cm^{-1}) and amide A (3400 cm^{-1} → 3446 cm^{-1}), decrease in absorbance at 1632 cm^{-1} and increase in the absorbance at 1655 cm^{-1}, disappearance of the IR peak at 1677 cm^{-1}, and no observation of the CD

Table 3. Hydrogelation properties of **1b–3b** in aqueous solutions containing acids and salts at 25 °C[a,b]

	Saline[c]	HCl	H_2SO_4	H_3PO_4	CH_3CO_2H	NaCl	KCl	$MgCl_2$	$CaCl_2$
1b	Ins	Ins	Ins	Ins	2	Ins	Ins	Ins	Ins
2b	3	4	3	5	5	8	8	8	P
3b	3	4	2	0.8	1	2	2	3	4

[a] Values denote MGC.
[b] Acids and salts are 1.0 M.
[c] Saline contains 8.6 g L^{-1} (ca. 0.147 M) NaCl, 0.3 g L^{-1} (ca. 4.02×10^{-3} M) KCl and 0.33 g L^{-1} (ca. 2.97×10^{-3} M) $CaCl_2$. Ins: insoluble and P: precipitate after dissolution.

Table 2. Hydrogelation properties of **1b–3b** in aqueous solutions with various pHs at 25 °C[a,b]

	0	1	2	3	4	5	6	7	8	9	10	11	12	13	14
1b	Ins	Ins	5	15	15	15	15	15	15	15	15	S	Ins	Ins	Ins
2b	4	8	10	10	10	10	3	5	10	10	10	P	P	S	S
3b	4	1	0.5	0.5	0.5	0.5	0.5	0.5	0.5	2	2	2	3	S	S

[a] Values denote minimum gel concentration (MGC, g L^{-1}).
[b] Aqueous solutions with various pHs were adjusted by HCl or NaOH: pH=0–6 by HCl, pH=8–10 by NaOH, and pH=7 is pure water. Ins: insoluble, P: precipitate after dissolution, and S: solution.

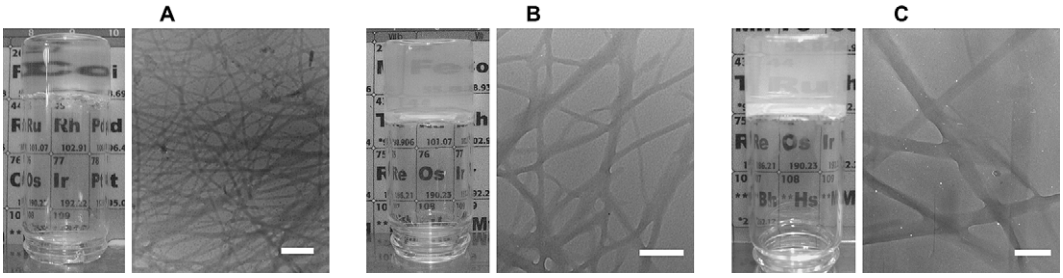

Figure 2. Photographs of hydrogels and TEM images of their dried gels. (A) pure water (0.5 g L^{-1}); (B) saline (3 g L^{-1}); and (C) 1 M NaCl (2 g L^{-1}) of **3b**. Scale bars are 200 nm.

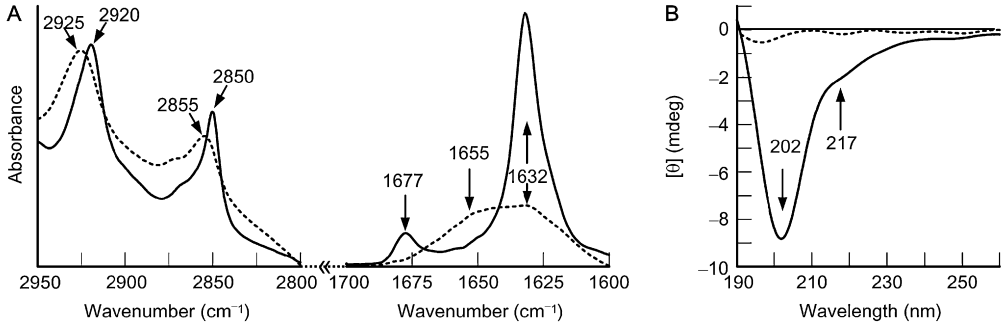

Figure 3. FTIR (A) and CD (B) spectra of D_2O gel (25 °C, solid line) and D_2O solution (80 °C, dashed line) of **3b** (5 g L^{-1}).

peak. Therefore, the nanofibers are formed through hydrophobic interaction and the intermolecular hydrogen bonding with an antiparallel β-sheet arrangement, and then a three-dimensional network is created by entanglement of the nanofibers, which leads to hydrogelation.

In order to obtain further information on the hydrogelation mechanism, we measured the FTIR spectra at various temperatures. Figure 4 shows the temperature dependences of the IR peak of the amide A and hydroxyl group region (A), ν_{as}C–H (B) as well as ν_sC–H (C), and absorbances at 1677 cm^{-1} (D) and 1632 cm^{-1} (E) in the D_2O gel of **3b**. Here, the IR spectra observed in this region (3400 cm^{-1}–3440 cm^{-1}) were likely conjugated by some spectra, e.g., νO–H (in gelator and of H_2O in D_2O), νN–H, etc, and the T_{gel} was 65 °C under the experimental conditions (10 g L^{-1}). The temperature dependences of the IR peaks of the amide groups were slightly different from those of the alkyl group. In the region of 3400 cm^{-1}–3440 cm^{-1}, the drastic changes were observed at 35 °C–45 °C and 63 °C–65 °C. The absorbances of the amide I changed at 60 °C–65 °C. In contrast, the IR bands of the νC–H changed at 65 °C–70 °C. These facts let us to propose the mechanism of the gel–sol transition as follows: the hydrogen bonding

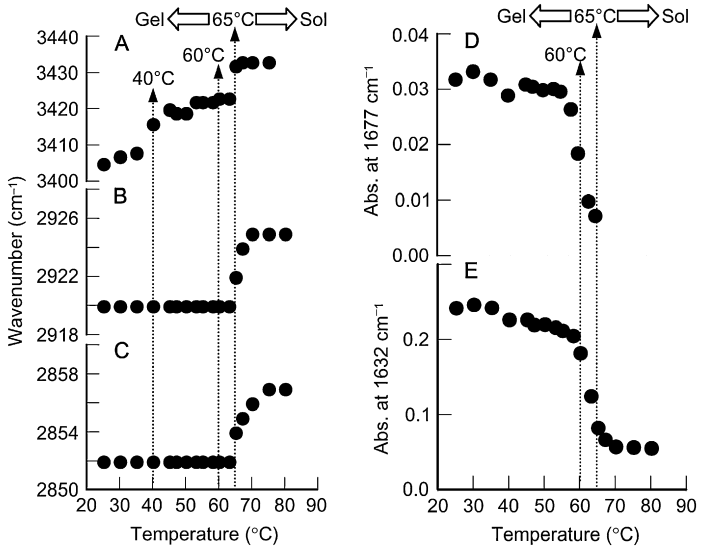

Figure 4. Temperature dependences of IR peaks obtained from VT–IR spectra of D_2O gel based on **3b** (5 g L^{-1}). (A) IR peak appearing in 3400–3440 cm^{-1}, (B) IR peak arising from ν_{as}C–H, (C) IR peak arising from ν_sC–H, (D) absorbance at 1677 cm^{-1}, and (E) absorbance at 1632 cm^{-1}. T_{gel} is 65 °C.

interactions of hydroxyl groups and amide groups are broken at 35 °C–45 °C and at 63 °C–65 °C, respectively, and around 65 °C, the gel state should be maintained by only hydrophobic interaction. Over 65 °C, the hydrophobic interaction is broken, leading to the destruction of the hydrogel.

In order to elucidate the excellent hydrogelation ability and thermal stability, some measurements were carried out. Gel strength is one of the important factors in the applications of hydrogels. In the present study, the gel strengths were evaluated as the power necessary to sink a cylindrical bar (10 mm in diameter) 4 mm deep in the hydrogels. As listed in Table 4, among three hydrogels, the pure water gel showed the largest gel strength and the value was 35 kPa. It is likely that the gel strength is connected with the rigidity of self-assembled nanofibers; namely, the gel strength of a hydrogel having a three-dimensional network formed by rigid nanofibers is large.[39] As shown in Figure 2, the sizes of nanofibers are the order of pure water gel<saline gel<1 M NaCl gel, while the gel strengths show the inverted order (pure water gel>saline gel>NaCl gel). Compound **3b** would form the narrower nanofibers and a more effective interpenetrated network, which leads to the large gel strength.

Figure 5 shows the gel–sol transition temperatures (T_{gel}) of pure water gel, saline gel, and 1 M NaCl gel based on **3b** as a function of the gelator concentrations. For the pure water gel, the T_{gel} values sharply increased to 65 °C with the increasing concentration of **3b** up to 5 g L^{-1}, and over 65 °C, **3b** was not able to gel pure water even at 50 g L^{-1}. The saline gel and 1 M NaCl gel had thermal stabilities and were maintained at 70 °C; 20 g L^{-1} for saline gel and 10 g L^{-1} for NaCl gel. These results indicate that **3b** forms thermally stable hydrogel in various aqueous solutions. It is noteworthy that the pure water gel formed by **3b** at 5 g L^{-1} has the highest T_{gel} (65 °C).

Table 4. Physical parameters for hydrogels based on **3b**[a]

	Pure water	Saline[b]	NaCl 1 M
T_{gel} (°C)	65	60	65
ΔH_{gel} (kJ mol^{-1})	81.5	99.3	107.2
Gel strength (kPa)	35.4	24.7	20.9

[a] [**3b**]=5 g L^{-1}.
[b] Saline contains 8.6 g L^{-1} (ca. 0.147 M) NaCl, 0.3 g L^{-1} (ca. 4.02×10^{-3} M) KCl, and 0.33 g L^{-1} (ca. 2.97×10^{-3} M) $CaCl_2$.

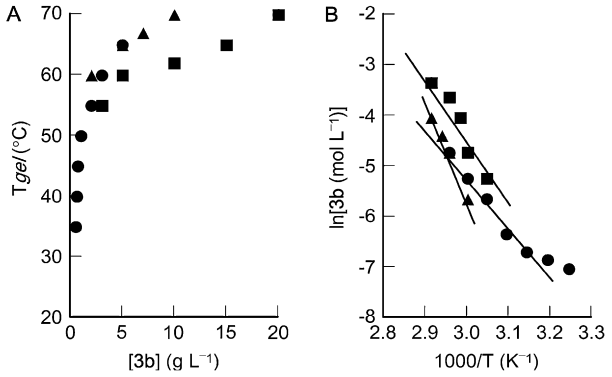

Figure 5. Dependence of T_{gel} on concentration of **3b** (A) and van't Hoff plots (B) for pure water gel (●), saline gel (■), and 1 M NaCl gel (▲).

The thermodynamic analysis for the gel–sol transition was carried out using a van't Hoff relationship.[40] From the relationship between T_{gel} and MGC, the gel–sol transition enthalpy (ΔH_{gel}) was determined from the slope of ln[**3b**] versus $(T_{gel})^{-1}$. For all hydrogels, the plots gave a linear relationship. The ΔH_{gel} values increased in the order of pure water gel<saline gel<1 M NaCl gel. This order reflects the concentration of inorganic salts in the aqueous solutions and size of the nanofibers. Because the ΔH_{gel} values are relative to the strength of intermolecular interactions (mainly hydrophobic interaction) in the nanofiber, the highest ΔH_{gel} value in 1 M NaCl solution of compound **3b** is caused by the strong intermolecular interactions.

3. Conclusion

In this paper, we revealed the easy synthesis and hydrogelation property of new L-lysine-based hydrogelators with glucoheptonamide. All L-lysine derivatives with a gluconic group have no hydrogelation ability, while the L-lysine derivatives of glucoheptonamide function as hydrogelators. The hydrogelation ability significantly depends on the length of spacer between the L-lysine segment and glucoheptonic group and increases with decreasing length. Especially, compound **3b**, which has no spacer, functions as a super hydrogelator that forms a hydrogel at 0.05 wt % in pure water, which corresponds to the immobilization of more than 62,000 water molecules per gelator molecule. The hydrogels based on **3b** have thermal stability and high mechanical strength. The FTIR studies demonstrate that the hydrogel is formed by the creation of a three-dimensional network through hydrogen bonding and hydrophobic interactions; particularly, the hydrophobic interaction plays an important role in the thermal stability of the hydrogel.

4. Experimental

4.1. General

4.1.1. Materials. N^{ε}-Lauroyl-L-lysine was obtained form Ajimonoto Co., Inc. The ethyl ester of N^{ε}-lauroyl-L-lysine was prepared according to the literature.[9] The other chemicals were of the highest commercial grade available and used without further purification. All solvents used in the syntheses were purified, dried, or freshly distilled as required.

4.1.2. Typical synthetic procedure.[41] To a stirring methanol suspension (20 mL) of D-glucono-1,5-lactone or D-glucoheptono-1,4-lactone (20 mmol), a methanol solution (50 mL) of amino acid derivatives with an amino group at the terminal (20 mmol) was carefully added dropwise at 50 °C. The reaction was continued for another 6 h. The reaction mixture was cooled to room temperature and then filtered to remove traces of unreacted lactone. The filtrate was evaporated to dryness. The crude solid was purified twice by recrystallization from methanol. The compounds **1a–3a** and **1b–3b** were obtained as white solids.

4.1.2.1. N^{α}-(12-Gluconamide-1-dodecanoyl)-N^{ε}-lauroyl-L-lysine ethyl ester (1a). Yield 93%. Mp= 120 °C–122 °C. IR (KBr): 3322, 1733, 1640, 1542 cm^{-1}.

^{1}H NMR (400 MHz, DMSO-d_6, TMS): 0.85 (t, J=6.6 Hz, 3H), 1.15–1.27 (m, 40H; alkyl), 1.33–1.46 (m, 8H), 1.52–1.71 (m, 2H), 2.02 (t, J=7.3 Hz, 2H), 3.02 (q, J=6.1 Hz, 2H), 3.02–3.08 (m, 2H), 3.30–3.39 (m, 1H), 3.45–3.48 (m, 2H), 3.53–3.56 (m, 1H), 3.66–3.67 (m, 1H), 3.85 (br, 1H), 3.92 (t, J=5.8 Hz, 1H), 4.02–4.11 (m, 1H), 4.12–4.17 (m, 1H), 4.28 (br, 1H), 4.36 (d, J=6.3 Hz, 1H), 4.43 (t, J=5.6 Hz, 1H), 4.84 (d, J=4.1 Hz, 1H), 5.48 (d, J=6.1 Hz, 1H), 7.72 (t, J=5.3 Hz, 1H), 7.84 (t, J=5.8 Hz, 1H), 8.10 (d, J=7.4 Hz, 1H). Elemental Anal. Calcd for $C_{38}H_{73}N_3O_{10}$ (732.00): C, 62.35; H, 10.05; N, 5.74. Found: C, 62.58; H, 10.33; N, 5.77.

4.1.2.2. N^{α}-(6-Gluconamide-1-hexanoyl)-N^{ε}-lauroyl-L-lysine ethyl ester (2a). Yield 89%. Mp=153 °C–154 °C. IR (KBr): 3327, 1731, 1644, 1544 cm^{-1}. ^{1}H NMR (400 MHz, DMSO-d_6, TMS): 0.85 (t, J=6.6 Hz, 3H), 1.15–1.35 (m, 24H; alkyl), 1.35–1.50 (m, 8H), 1.51–1.69 (m, 2H), 2.02 (t, J=7.3 Hz, 2H), 2.10 (t, J=7.3 Hz, 2H), 2.91–3.02 (m, 2H), 3.05–3.09 (m, 2H), 3.34–3.40 (m, 1H), 3.48 (br, 2H), 3.55–3.61 (m, 1H), 3.90 (br, 1H), 3.97 (t, J=4.3 Hz, 1H), 4.03–4.10 (m, 1H), 4.11–4.17 (m, 1H), 4.31 (t, J=5.6 Hz, 1H), 4.37 (d, J=4.4 Hz, 1H), 4.45 (d, J=4.5 Hz, 1H), 4.51 (d, J=4.5 Hz, 1H), 5.32 (d, J=4.8 Hz, 1H), 7.58 (t, J=5.8 Hz, 1H), 7.71 (t, J=5.6 Hz, 1H), 8.08 (d, J=7.3 Hz, 1H). Elemental Anal. Calcd for $C_{32}H_{61}N_3O_{10}$ (647.84): C, 59.33; H, 9.49; N, 6.49. Found: C, 59.77; H, 9.71; N, 6.52.

4.1.2.3. N^{α}-(12-Glucoheptonamide-1-dodecanoyl)-N^{ε}-lauroyl-L-lysine ethyl ester (1b). Yield 91%. Mp=117 °C–119 °C. IR (KBr): 3311, 1740, 1639, 1546 cm^{-1}. ^{1}H NMR (400 MHz, DMSO-d_6, TMS): 0.85 (t, J=6.6 Hz, 3H), 1.15–1.27 (m, 40H; alkyl), 1.34–1.48 (m, 8H), 1.53–1.73 (m, 2H), 2.02 (t, J=7.3 Hz, 2H), 3.00 (q, J=6.3 Hz, 2H), 3.04–3.10 (m, 2H), 3.31–3.39 (m, 1H), 3.45–3.48 (m, 2H), 3.55–3.58 (m, 1H), 3.66–3.67 (m, 1H), 3.85 (br, 1H), 3.92 (t, J=5.8 Hz, 1H), 4.02–4.11 (m, 2H), 4.12–4.17 (m, 1H), 4.28 (br, 1H), 4.36 (d, J=6.3 Hz, 1H), 4.43 (t, J=5.6 Hz, 2H), 4.81 (d, J=4.1 Hz, 1H), 5.45 (d, J=6.1 Hz, 1H), 7.71 (t, J=5.3 Hz, 1H), 7.81 (t, J=5.8 Hz, 1H), 8.06 (d, J=7.4 Hz, 1H). Elemental Anal. Calcd for $C_{39}H_{75}N_3O_{11}$ (762.03): C, 61.47; H, 9.92; N, 5.51. Found: C, 61.49; H, 9.99; N, 5.53.

4.1.2.4. N^{α}-(6-Glucoheptonamide-1-hexanoyl)-N^{ε}-lauroyl-L-lysine ethyl ester (2b). Yield 88%. Mp=150 °C–153 °C. IR (KBr): 3314, 1723, 1639, 1559 cm^{-1}. ^{1}H NMR (400 MHz, DMSO-d_6, TMS): 0.85 (t, J=6.8 Hz, 3H), 1.15–1.27 (m, 24H; alkyl), 1.35–1.52 (m, 8H), 1.53–1.66 (m, 2H), 2.02 (t, J=7.1 Hz, 2H), 2.10 (t, J=7.4 Hz, 2H), 3.00 (q, J=6.3 Hz, 2H), 3.07 (q, J=7.1 Hz, 2H), 3.34–3.38 (m, 1H), 3.43–3.51 (br, 2H), 3.53–3.61 (m, 1H), 3.66–3.69 (m, 1H), 3.84–3.87 (m, 1H), 3.92 (t, J=6.3 Hz, 1H), 4.03–4.10 (m, 2H), 4.11–4.17 (m, 1H), 4.28 (t, J=5.8 Hz, 1H), 4.37 (d, J=6.6 Hz, 1H), 4.43 (q, J=2.1 Hz, 2H), 4.81 (d, J=6.8 Hz, 1H), 5.49 (d, J=6.6 Hz, 1H), 7.71 (t, J=5.6 Hz, 1H), 7.82 (t, J=5.8 Hz, 1H), 8.08 (d, J=7.6 Hz, 1H). Elemental Anal. Calcd for $C_{33}H_{63}N_3O_{11}$ (677.87): C, 58.47; H, 9.37; N, 6.20. Found: C, 58.79; H, 9.59; N, 6.24.

4.1.2.5. N^{α}-Gluconamide-N^{ε}-lauroyl-L-lysine ethyl ester (3a). Yield 95%. Mp=125 °C–127 °C. IR (KBr): 3401, 3316, 1739, 1643, 1547 cm^{-1}. ^{1}H NMR (400 MHz, DMSO-d_6, TMS): 0.88 (t, J=6.6 Hz, 3H), 1.25–1.31 (m, 21H; alkyl), 1.48–1.56 (m, 2H), 1.58–1.62 (m, 2H), 1.70–1.88 (m, 2H), 2.14 (t, J=7.3 Hz, 2H), 3.17 (q, J=6.0 Hz, 2H), 3.54 (br, 1H), 2.70–3.82 (m, 7H), 4.16–4.21 (m, 3H), 4.30 (d, J=3.6 Hz, 1H), 4.50–4.55 (m, 1H), 6.71 (t, J=5.3 Hz, 1H), 7.50 (d, J=8.1 Hz, 1H). Elemental Anal. Calcd for $C_{26}H_{50}N_2O_9$ (534.68): C, 58.40; H, 9.43; N, 5.24. Found: C, 58.55; H, 9.89; N, 5.25.

4.1.2.6. N^{α}-Glucoheptonamide-N^{ε}-lauroyl-L-lysine ethyl ester (3b). Yield 95%. Mp=114 °C–116 °C. IR (KBr): 3446, 3392, 3349, 3305, 1734, 1682, 1644, 1549 cm^{-1}. ^{1}H NMR (400 MHz, DMSO-d_6, TMS): 0.86 (t, J=6.6 Hz, 3H), 1.19 (t, J=7.1 Hz, 3H), 1.23 (br, 18H; alkyl), 1.33–1.38 (m, 2H), 1.42–1.50 (m, 2H), 1.60–1.75 (m, 2H), 2.02 (t, J=7.3 Hz, 2H), 2.96–2.99 (m, 2H), 3.31 (br, 2H), 3.34–3.39 (m, 1H), 3.44–3.49 (m, 2H), 3.87–3.89 (m, 1H), 3.98 (t, J=6.6 Hz, 1H), 4.06–4.12 (m, 2H), 4.21–4.25 (m, 1H), 4.28–4.30 (m, 2H), 4.42–4.45 (m, 2H), 4.66 (d, J=4.8 Hz, 1H), 5.43 (d, J=6.6 Hz, 1H), 7.69 (t, J=5.6 Hz, 1H), 7.99 (d, J=7.6 Hz, 1H). Elemental Anal. Calcd for $C_{27}H_{52}N_2O_{10}$ (564.71): C, 57.43; H, 9.28; N, 4.96. Found: C, 57.64; H, 9.49; N, 4.98.

4.1.3. Apparatus for measurements. The elemental analyses were performed using a Perkin–Elmer series II CHNS/O analyzer 2400. The FTIR spectra were recorded on a JASCO FS-420 spectrometer. The TEM observations were carried out using a JEOL JEM-2010 electron microscope at 200 kV. The ^{1}H NMR spectra were measured using a Bruker AVANCE 400 spectrometer. The gel strengths of the hydrogels were measured using a Sun Science Sun Rheo Meter CR-500DX. The circular dichroism spectra were measured using a JASCO Circular Dichroism J-600 spectrometer.

4.1.4. Gelation test. A mixture of a weighed gelator in solvent (1 mL) in a sealed test tube was heated until a clear solution appeared. After allowing the solutions to stand at 25 °C for 6 h, the state of the solution was evaluated by the 'test tube inversion' method.

4.1.5. Transmission electron microscope (TEM). The samples were prepared as follows: aqueous solutions of the gelators were added dropwise onto a collodion- and carbon-coated 400 mesh copper grid. The grids were then dried under vacuum for 24 h. The dried samples were stored in a sealed bottle containing osmic oxide in acetone overnight.

4.1.6. Gel strength. Samples were prepared as follows: a mixture of a weighed gelator in water (2 mL) in a sealed sample tube (15 mm in diameter) was heated until a clear solution appeared. The resulting solution was allowed to stand at 25 °C for 6 h. The gel strength was evaluated as the force necessary to sink a cylinder bar (10 mm in diameter) 4 mm deep in the gel.

4.1.7. FTIR study. The FTIR spectroscopy was performed using the spectroscopic cell with a CaF_2 window and 50 mm spacers operating at a 2 cm^{-1} resolution with 32 scans.

4.1.8. Temperature-controlled FTIR study. An automatic temperature-control cell unit (Specac Inc., P/N 20,730) with

a vacuum-tight liquid cell (Specac Inc., P/N 20,502, path length 50 μm) fitted with CaF_2 windows was used to measure the IR spectra at different temperatures.

4.1.9. Circular dichroism. The CD spectra were measured for the D_2O gel at 25 °C and the solution state at 80 °C of **3b**.

Acknowledgements

This work was supported by a Grant-in-aid for the 21st century COE Program and a Grant-in-aid for Exploratory Research (No. 17655049) by Ministry of Education, Sports, Culture, Science, and Technology of Japan and by Tokuyama Science Foundation.

Supplementary data

Supplementary data associated with this article can be found in the online version, at doi:10.1016/j.tet.2007.02.065.

References and notes

1. *Low Molecular Mass Gelators*; Fages, F., Ed.; Topics in Current Chemistry; Springer: Berlin, Heidelberg, 2005; Vol. 256.
2. Estroff, L. A.; Hamilton, A. D. *Chem. Rev.* **2004**, *104*, 1201–1217.
3. de Loos, M.; Feringa, B. L.; van Esch, J. H. *Eur. J. Org. Chem.* **2005**, 3615–3631.
4. Terech, P.; Weiss, R. G. *Chem. Rev.* **1997**, *97*, 3133–3159.
5. *Molecular Gels: Materials with Self-assembled Fibrillar Networks*; Weiss, R. G., Terech, P., Eds.; Springer: Dordrecht, 2006.
6. Estroff, L. A.; Hamilton, A. D. *Angew. Chem., Int. Ed.* **2000**, *39*, 3447–3450.
7. Menger, F. M.; Caran, K. L. *J. Am. Chem. Soc.* **2000**, *122*, 11679–11691.
8. Bhattacharya, S.; Acharya, S. N. G. *Langmuir* **2000**, *16*, 87–97.
9. Suzuki, M.; Yumoto, M.; Kimura, M.; Shirai, H.; Hanabusa, K. *Chem. Commun.* **2002**, 884–885.
10. Jung, J. H.; John, G.; Masuda, M.; Yoshida, K.; Shinkai, S.; Shimizu, T. *Langmuir* **2001**, *17*, 7229–7232.
11. Gronwald, O.; Shinkai, S. *J. Chem. Soc., Perkin Trans. 2* **2001**, 1933–1937.
12. Makarević, J.; Jokić, M.; Perić, B.; Tomišić, V.; Kojić-Prodić, B.; Žinić, M. *Chem.—Eur. J.* **2001**, *7*, 3328–3341.
13. Wang, G.; Hamilton, A. D. *Chem. Commun.* **2003**, 310–311.
14. Kobayashi, H.; Friggeri, A.; Koumoto, K.; Amaike, M.; Shinkai, S.; Reinhoudt, D. N. *Org. Lett.* **2002**, *4*, 1423–1426.
15. Heeres, A.; van der Pol, C.; Stuart, M.; Friggeri, A.; Feringa, B. L.; van Esch, J. *J. Am. Chem. Soc.* **2003**, *125*, 14252–14253.
16. Kiyonaka, S.; Sada, K.; Yoshimura, I.; Shinkai, S.; Kato, N.; Hamachi, I. *Nat. Mater.* **2004**, *3*, 58–64.
17. Bhuniya, S.; Park, S. M.; Kim, B. H. *Org. Lett.* **2005**, *7*, 1741–1744.
18. Karinaga, R.; Jeong, Y.; Shinkai, S.; Kaneko, J.; Sakurai, K. *Langmuir* **2005**, *21*, 9398–9401.
19. Srivastave, A.; Ghorai, S.; Bhattacharjya, A.; Bhattacharya, S. *J. Org. Chem.* **2005**, *70*, 6574–6582.
20. Köhler, K.; Meister, A.; Förster, G.; Dobner, B.; Drescher, S.; Ziethe, F.; Richer, W.; Steiniger, F.; Drechsler, M.; Hause, G.; Blume, A. *Soft Matter* **2006**, *2*, 77–86.
21. Yang, Z.; Liang, G.; Xu, B. *Chem. Commun.* **2006**, 738–740.
22. Suzuki, M.; Yumoto, M.; Kimura, M.; Shirai, H.; Hanabusa, K. *Chem. Lett.* **2004**, *33*, 1496–1497.
23. Suzuki, M.; Yumoto, M.; Kimura, M.; Shirai, H.; Hanabusa, K. *Chem.—Eur. J.* **2003**, *9*, 348–354.
24. Suzuki, M.; Owa, S.; Yumoto, M.; Kimura, M.; Shirai, H.; Hanabusa, K. *Tetrahedron Lett.* **2004**, *45*, 5399–5402.
25. Suzuki, M.; Owa, S.; Kimura, M.; Kurose, A.; Shirai, H.; Hanabusa, K. *Tetrahedron Lett.* **2005**, *46*, 303–306.
26. Suzuki, M.; Nanbu, M.; Yumoto, M.; Shirai, H.; Hanabusa, K. *New J. Chem.* **2005**, *29*, 1439–1444.
27. Shimizu, T.; Masuda, M.; Minamikawa, H. *Chem. Rev.* **2005**, *105*, 1401–1443.
28. Tamaru, S.; Kiyonaka, S.; Hamachi, I. *Chem.—Eur. J.* **2005**, *11*, 7294–7304.
29. Dhruv, H. D.; Draper, M. A.; Britt, D. W. *Chem. Mater.* **2005**, *17*, 6239–6245.
30. Jung, J. H.; Shinkai, S.; Shimizu, T. *Chem.—Eur. J.* **2002**, *8*, 2684–2690.
31. Iwaura, R.; Yoshida, K.; Masuda, M.; Yase, K.; Shimizu, T. *Chem. Mater.* **2002**, *14*, 3047–3053.
32. Fuhrhop, J. H.; Schneider, P.; Rosenberg, J.; Boekema, E. *J. Am. Chem. Soc.* **1987**, *109*, 3387–3390.
33. Fuhrhop, J. H.; Wang, T. *Chem. Rev.* **2004**, *104*, 2901–2937.
34. Bhuniya, S.; Kim, B. H. *Chem. Commun.* **2006**, 1842–1844.
35. Montalti, M.; Dolci, L. S.; Prodi, L.; Zaccheroni; Stuart, M. C. A.; van Bommel, K. J. C.; Friggeri, A. *Langmuir* **2006**, *22*, 2299–2303.
36. See Supplementary data.
37. Koga, T.; Higuchi, M.; Kinoshita, T.; Higashi, N. *Chem.—Eur. J.* **2006**, *12*, 1360–1367.
38. Lamm, M. S.; Rajagopal, K.; Schneider, J. P.; Pochan, D. J. *J. Am. Chem. Soc.* **2005**, *127*, 16692–16700.
39. Suzuki, M.; Yumoto, M.; Kimura, M.; Shirai, H.; Hanabusa, K. *Tetrahedron Lett.* **2004**, *45*, 2947–2950.
40. Seo, S. H.; Chang, J. Y. *Chem. Mater.* **2005**, *17*, 3249–3254.
41. Piłakowska-Pietras, D.; Lunkheimer, K.; Piasecki, A.; Pietras, M. *Langmuir* **2005**, *21*, 4016–4023.